Synchronising chaotic Chua's circuit using switching feedback control based on piecewise quadratic Lyapunov functions*

Zhang Hong-Bin(张洪斌)[a)d)], Xia Jian-Wei(夏建伟)[b)],
Yu Yong-Bin(于永斌)[c)], and Dang Chuang-Yin(党创寅)[d)]

[a)] *School of Electronic Engineering, University of Electronic Science and Technology of China, Chengdu* 610054, *China*
[b)] *School of Mathematics Science, Liaocheng University, Liaocheng* 252000, *China*
[c)] *School of Computer Science & Engineering, University of Electronic Science and Technology of China, Chengdu* 610054, *China*
[d)] *Manufacturing Engineering & Engineering Management, City University of Hong Kong, Kowloon, Hong Kong*

(Received 4 September 2008; revised manuscript received 9 July 2009)

This paper investigates the chaos synchronisation between two coupled chaotic Chua's circuits. The sufficient condition presented by linear matrix inequalities (LMIs) of global asymptotic synchronisation is attained based on piecewise quadratic Lyapunov functions. First, we obtain the piecewise linear differential inclusions (pwLDIs) model of synchronisation error dynamics, then we design a switching (piecewise-linear) feedback control law to stabilise it based on the piecewise quadratic Laypunov functions. Then we give some numerical simulations to demonstrate the effectiveness of our theoretical results.

Keywords: chaos, Chua's circuit, piecewise quadratic Lyapunov functions, synchronisation
PACC: 0545

1. Introduction

Since the early 1990s researchers have realised that chaotic systems can be synchronized.[1,2] Increasing interest has been generated in chaotic synchronisation and its practical applications in different fields, particularly in communications because chaotic systems are deterministic but extremely sensitive to initial conditions and have noise-like behaviour.[3−20] According to Ref. [2], the problem of chaotic synchronisation is defined such that under given different initial conditions between drive and response systems, it is possible to find a method to make the states of drive and response systems achieve synchrony. Many theories[6,7,21,22] have been proposed to achieve the synchronized manner from drive-response configuration. This drive-response configuration consists of the original chaotic system as a *drive system* to provide a *driving signal* to drive another system called the *response system* to synchrony. There are two main approaches for this synchronisation problem: consider the synchronisation as an observer design problem[21,22] and consider it as a tracking control problem,[6,23−27] in which the response system can track the drive system asymptotically. Due to the simple configuration and ease of implementation in real systems, the feedback scheme is especially attractive and adopted for practical implementation.[3] For this reason, chaos synchronisation using feedback control is studied in this paper.

On the other hand, piecewise-linear systems have been a subject of research in circuits and control system community for some time, (see Refs. [18]–[31] and the references therein). Chua's circuit has become a standard prototype to study the dynamics of nonlinear circuits because Chua's circuit is a simple system that exhibits a wide variety of nonlinear dynamics phenomena such as bifurcations and chaos. It is well known that Chua's circuit contains only a nonlinear component which is a piecewise linear resistor,[32] that is to say, Chua's circuit is actually a piecewise linear system. According to Ref. [22], the observer can be easily designed for synchronisation based on standard linear poleplacement techniques, but both the outputs of dynamic system and observer are strictly restricted in order to cancel all the nonlinear terms exactly. In

*Project partially supported by the grant from the Research Grants Council of the Hong Kong Special Administrative Region, China (Grant No. 101005), the National Natural Science Foundation of China (Grant No. 60904004), the Key Youth Science and Technology Foundation of University of Electronic Science and Technology of China (Grant No. L08010201JX0720).
†Corresponding author. E-mail: zhanghb@uestc.edu.cn
© 2010 Chinese Physical Society and IOP Publishing Ltd

this paper, we study the synchronisation problem of two coupled chaotic Chua's circuits (drive-response configuration) based on piecewise quadratic Lyapunov function.[33−37] According to the object of chaos synchronisation, we first found the exact piecewise linear differential inclusions (pwLDIs) model of the synchronisation error dynamics for the chaos synchronisation of Chua's circuits, and then the piecewise-linear error feedback strategy is adopted due to the property of the error dynamics in order to obtain a lower feedback gain. The sufficient global stabilization condition is presented by LMI's.[38] It has less conservation because the proper piecewise quadratic Lyapunov function is searched for controlled synchronisation error dynamics. Finally, a simpler ILMI (iterative linear matrix inequality) algorithm is used to find the switching feedback control gain of stabilization.

The rest of this paper is organized as follows. In the next section, preliminaries are presented. In Section 3, we give theoretical analysis and results. Simulation examples are given in Section 4. Finally, we draw conclusions in Section 5.

2. Preliminaries

2.1. Chua's circuit

Chua's circuit is a simple and interesting electronic system which consists of one inductor, two capacitors and one piecewise-linear nonlinear resistor, as shown in Fig. 1.

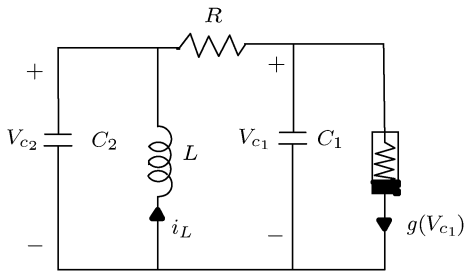


Fig. 1. Chua's circuit.

In the figure, L is an inductor, C_1, C_2 are two capacitors, g is a 3-segment piecewise-linear resistor, R is a linear resistor.

The circuit dynamics is described by

$$\begin{cases} C_1 \dfrac{\mathrm{d}v_{C_1}}{\mathrm{d}t} = \dfrac{1}{R}(v_{C_2} - v_{C_1}) - g(v_{C_1}), \\ C_2 \dfrac{\mathrm{d}v_{C_2}}{\mathrm{d}t} = \dfrac{1}{R}(v_{C_1} - v_{C_2}) + i_L, \\ L \dfrac{\mathrm{d}i_L}{\mathrm{d}t} = -v_{C_2}, \end{cases} \tag{1}$$

where C_1, C_2, L, and R are all circuit parameters, i_L is the current through the inductor L, v_{C_1} and v_{C_2} are the voltages across C_1 and C_2, respectively, and the piecewise linear function $g(v_C)$ describes the $v-i$ characteristics of the Chua's diode g as follows:

$$g(v_{C_1}) = m_0 v_{C_1} + \frac{1}{2}(m_1 - m_0) \times (|v_{C_1} + B_p| - |v_{C_1} - B_p|). \tag{2}$$

Via the resealing, we have $x_1 = v_{C_1}/B_p$, $x_2 = v_{C_2}/B_p$, $x_3 = i_L R/B_p$, $\tau = t/C_2R$, $a = m_1 R$, $b = m_0 R$, $p = C_2/C_1$, $q = C_2R^2/L$, and $B_p = 1$. Equation (1) is transformed into the following simpler dimensionless form

$$\begin{cases} \dot{x_1}(\tau) = p(x_2 - x_1 - f(x_1)), \\ \dot{x_2}(\tau) = x_1 - x_2 + x_3, \\ \dot{x_3}(\tau) = -q x_2, \end{cases} \tag{3}$$

where $f(x_1)$ is a piecewise linear function represented by

$$f(x_1) = \begin{cases} bx_1 + a - b, & x_1 \geq 1, \\ ax_1, & |x_1| \leq 1, \\ bx_1 - a + b, & x_1 \leq -1. \end{cases} \tag{4}$$

It is known that when the values of the system parameters (p, q, a, b) are chosen to be (9, 100/7, −8/7, −5/7), a typical chaotic attractor (a double scroll) can be found in dynamical system (3).[32]

2.2. Piecewise linear system and stability

Before discussing the synchronisation issue of Chua's circuit, we first introduce the piecewise linear system model and its stability. According to Ref. [34], piecewise linear system has the following form

$$\dot{\boldsymbol{x}}(t) = \boldsymbol{A}_l \boldsymbol{x}(t) + \boldsymbol{\alpha}_l, \quad \text{for} \quad \boldsymbol{x}(t) \in \boldsymbol{X}_l. \tag{5}$$

Here, $\boldsymbol{x}(t) \in \boldsymbol{R}^n$, α_l is affine term, $\{\boldsymbol{X}_l\}_{l \in L} \subseteq \boldsymbol{R}^n$ is a partition of the state space into a number of closed (possibly unbounded) polyhedral cells with pairwise disjoint interior. The index set of the cells is denoted L. Let $\boldsymbol{x}(t) \in \bigcup_{l \in L} \boldsymbol{X}_l$ be a continuous piecewise C^1 function on the time interval $[0, T]$. We say that

$\boldsymbol{x}(t)$ is a trajectory of Eq. (5), if for every $t \in [0,T]$ such that the derivative $\dot{\boldsymbol{x}}(t)$ is defined, the equation $\dot{\boldsymbol{x}}(t) = \boldsymbol{A}_l\boldsymbol{x}(t) + \boldsymbol{\alpha}_l$ holds for all l with $\boldsymbol{x}(t) \in \boldsymbol{X}_l$. Let $L_0 \subseteq L$ be the index set for cells that contain origin, and let $L_1 = L \backslash L_0$. It is assumed that $\boldsymbol{\alpha}_l = \boldsymbol{0}$ for $l \in L_0$. For convenient notation, we introduce

$$\bar{\boldsymbol{A}}_l = \begin{bmatrix} \boldsymbol{A}_l & \boldsymbol{a}_l \\ 0 & 0 \end{bmatrix}. \tag{6}$$

As shown in Ref. [33], in order to find the piecewise Lyapunov function continuous across cell boundaries, the following matrices $\bar{\boldsymbol{F}}_l = [\boldsymbol{F}_l \quad \boldsymbol{f}_l]$, $l \in L$ with $f_l = 0$ for $l \in L_0$ need to be constructed, which is used to characterise the boundary among cells.

$$\bar{\boldsymbol{F}}_l \begin{bmatrix} \boldsymbol{x} \\ 1 \end{bmatrix} = \bar{\boldsymbol{F}}_j \begin{bmatrix} \boldsymbol{x} \\ 1 \end{bmatrix}, \quad \boldsymbol{x} \in \boldsymbol{X}_l \cap \boldsymbol{X}_j, \quad l,j \in L. \tag{7}$$

In addition, to reduce the conservation of the stability result, the S-procedure has been used in Ref. [33]. To this end, one can construct matrices, $\bar{\boldsymbol{E}}_l = [\boldsymbol{E}_l \quad \boldsymbol{e}_l]$, $l \in L$ with $\boldsymbol{e}_l = \boldsymbol{0}$ for $l \in L_0$ such that

$$\bar{\boldsymbol{E}}_l \begin{bmatrix} \boldsymbol{x} \\ 1 \end{bmatrix} \geq 0 \qquad \boldsymbol{x} \in \boldsymbol{X}_l, \quad l \in L. \tag{8}$$

The piecewise quadratic Lyapunov function candidates that are continuous across the subspace boundaries can be parameterised as

$$\boldsymbol{V}(x) = \begin{cases} \boldsymbol{x}^{\mathrm{T}}\boldsymbol{P}_l\boldsymbol{x}, & \boldsymbol{x} \in \boldsymbol{X}_l,\ l \in L_0; \\ \begin{bmatrix} \boldsymbol{x} \\ 1 \end{bmatrix}^{\mathrm{T}} \bar{\boldsymbol{P}}_l \begin{bmatrix} \boldsymbol{x} \\ 1 \end{bmatrix}, & \boldsymbol{x} \in \boldsymbol{X}_l,\ l \in L_1, \end{cases} \tag{9}$$

with

$$\begin{aligned} \boldsymbol{P}_l &= \boldsymbol{F}_l^{\mathrm{T}}\boldsymbol{T}\boldsymbol{F}_l, \quad l \in L_0; \\ \bar{\boldsymbol{P}}_l &= \bar{\boldsymbol{F}}_l^{\mathrm{T}}\boldsymbol{T}\bar{\boldsymbol{F}}_l, \quad l \in L_1, \end{aligned} \tag{10}$$

where the free parameters of the Lyapunov function candidates are characterised by the symmetric matrix $\boldsymbol{T}$. Now, we have the following stability result about piecewise linear system.

Lemma 1 Piecewise quadratic stability[33] Consider symmetric matrices $\boldsymbol{T}$ and $\boldsymbol{U}_l$ and $\boldsymbol{W}_l$, such that $\boldsymbol{U}_l$ and $\boldsymbol{W}_l$ have non-negative entries, while

$$\boldsymbol{P}_l = \boldsymbol{F}_l^T\boldsymbol{T}\boldsymbol{F}_l, \quad l \in L_0, \tag{11}$$

$$\bar{\boldsymbol{P}}_l = \bar{\boldsymbol{F}}_l^{\mathrm{T}}\boldsymbol{T}\bar{\boldsymbol{F}}_l, \quad l \in L_1, \tag{12}$$

satisfy

$$\begin{cases} 0 > \boldsymbol{A}_l^{\mathrm{T}}\boldsymbol{P}_l + \boldsymbol{P}_l\boldsymbol{A}_l + \boldsymbol{E}_l^{\mathrm{T}}\boldsymbol{U}_l\boldsymbol{E}_l, \\ 0 < \boldsymbol{P}_l - \boldsymbol{E}_l^{\mathrm{T}}\boldsymbol{W}_l\boldsymbol{E}_l, \end{cases} \quad l \in L_0; \tag{13}$$

$$\begin{cases} 0 > \bar{\boldsymbol{A}}_l^{\mathrm{T}}\bar{\boldsymbol{P}}_l + \bar{\boldsymbol{P}}_l\bar{\boldsymbol{A}}_l + \bar{\boldsymbol{E}}_l^{\mathrm{T}}\boldsymbol{U}_l\bar{\boldsymbol{E}}_l, \\ 0 < \bar{\boldsymbol{P}}_l - \bar{\boldsymbol{E}}_l^{\mathrm{T}}\boldsymbol{W}_l\bar{\boldsymbol{E}}_l, \end{cases} \quad l \in L_1. \tag{14}$$

Then every continuous piecewise C^1 trajectory $\boldsymbol{x}(t) \in \cup_{l\in L}\boldsymbol{X}_l$, satisfying Eq. (5) for $t \geq 0$, tends to zero exponentially.

Lemma 1 can be easily extended to systems described by piecewise linear differential inclusions (pwLDIs)

$$\dot{\boldsymbol{x}}(t) = \sum_{j=1}^{J} \lambda_{lj}(t)\left(\boldsymbol{A}_{lj}\boldsymbol{x}(t) + \boldsymbol{\alpha}_{lj}\right), \quad \boldsymbol{x}(t) \in \boldsymbol{X}_l. \tag{15}$$

We assume that for every t there exist scalars $\lambda_{lj}(t) \geq 0$ with $\sum\limits_j \lambda_{lj}(t) = 1$. For convenience, we associate an index set $J(l)$ to each cell $\boldsymbol{X}_l$ that specifies the j extreme dynamics $\dot{\boldsymbol{x}}(t) = \boldsymbol{A}_{lj}\boldsymbol{x}(t) + \boldsymbol{\alpha}_{lj}$, $j \in J(l)$ that define the inclusion in each cell and we have the following result.

Lemma 2 (Piecewise quadratic stability of pwLDIs[34] Consider symmetric matrices $\boldsymbol{T}$, $\boldsymbol{U}_{lj}$ and $\boldsymbol{W}_{lj}$, such that $\boldsymbol{U}_{lj}$ and $\boldsymbol{W}_{lj}$ have non-negative entries, while

$$\boldsymbol{P}_l = \boldsymbol{F}_l^{\mathrm{T}}\boldsymbol{T}\boldsymbol{F}_l, \quad (l \in L_0), \tag{16}$$

$$\bar{\boldsymbol{P}}_l = \bar{\boldsymbol{F}}_l^{\mathrm{T}}T\bar{\boldsymbol{F}}_l, \quad (l \in L_1) \tag{17}$$

satisfy

$$\begin{cases} 0 > \boldsymbol{A}_{lj}^{\mathrm{T}}\boldsymbol{P}_l + \boldsymbol{P}_l\boldsymbol{A}_{lj} + \boldsymbol{E}_l^{\mathrm{T}}\boldsymbol{U}_{lj}\boldsymbol{E}_l, \\ 0 < \boldsymbol{P}_l - \boldsymbol{E}_l^{\mathrm{T}}\boldsymbol{W}_{lj}\boldsymbol{E}_l, \end{cases} \quad l \in L_0, \quad j \in J(l); \tag{18}$$

$$\begin{cases} 0 > \bar{\boldsymbol{A}}_{lj}^{\mathrm{T}}\bar{\boldsymbol{P}}_l + \bar{\boldsymbol{P}}_l\bar{\boldsymbol{A}}_{lj} + \bar{\boldsymbol{E}}_l^{\mathrm{T}}\boldsymbol{U}_{lj}\bar{\boldsymbol{E}}_l, \\ 0 < \bar{\boldsymbol{P}}_l - \bar{\boldsymbol{E}}_l^{\mathrm{T}}\boldsymbol{W}_{lj}\bar{\boldsymbol{E}}_l, \end{cases} \quad l \in L_1, \quad j \in J(l). \tag{19}$$

Then every continuous piecewise C^1 trajectory $\boldsymbol{x}(t) \in \cup_{l\in L}\boldsymbol{X}_l$, satisfying Eq. (15) for $t \geq 0$, tends to zero exponentially.

3. Synchronising Chua's circuit

In this paper, we consider the drive-presponse configuration for synchronisation as shown in Fig. 2.

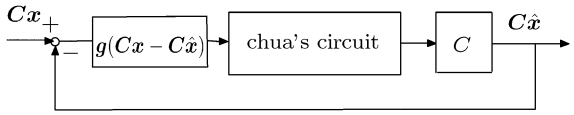


Fig. 2. Drive-response scheme for synchronisation. $\boldsymbol{Cx}$ and $\boldsymbol{C\hat{x}}$ are outputs of drive system and response system respectively.

Clearly, Chua's circuit is a typical piecewise linear system because Chua's circuit has only a nonlinear component which is piecewise-linear. Now, we present the dynamics of Chua's circuit in the following form with three cell partitions: $\boldsymbol{X}_1$: $\{(x_1, x_2, x_3)|x_1 \leq -1\}$, $\boldsymbol{X}_2$: $\{(x_1, x_2, x_3)||x_1| \leq 1\}$, and $\boldsymbol{X}_3 : \{(x_1, x_2, x_3)|x_1 \geq 1\}$, $\boldsymbol{X}_1 \bigcup \boldsymbol{X}_2 \bigcup \boldsymbol{X}_3 = \boldsymbol{R}^3$.

$$\begin{aligned} &\dot{\boldsymbol{x}}(t) = (\boldsymbol{A}_l\boldsymbol{x}(t) + \boldsymbol{\alpha}_l), \quad \boldsymbol{x}(t) \in \boldsymbol{X}_l, \quad l = 1, 2, 3; \\ &\boldsymbol{y}(t) = \boldsymbol{C}\boldsymbol{x}(t), \end{aligned} \tag{20}$$

where $\boldsymbol{x}(t) \in \boldsymbol{R}^3$ and $\boldsymbol{y}(t) \in \boldsymbol{R}^3$ are the state and output of the Chua's circuit respectively. $\boldsymbol{C} \in \boldsymbol{R}^{3\times 3}$ is an output constant matrix. In cell $\boldsymbol{X}_1$:

$$\boldsymbol{A}_1 = \begin{bmatrix} -p(b+1) & p & 0 \\ 1 & -1 & 1 \\ 0 & -q & 0 \end{bmatrix}, \quad \boldsymbol{\alpha}_1 = \begin{bmatrix} -p(b-a) \\ 0 \\ 0 \end{bmatrix}; \tag{21}$$

in cell $\boldsymbol{X}_2$:

$$\boldsymbol{A}_2 = \begin{bmatrix} -p(a+1) & p & 0 \\ 1 & -1 & 1 \\ 0 & -q & 0 \end{bmatrix}, \quad \boldsymbol{\alpha}_2 = \begin{bmatrix} 0 \\ 0 \\ 0 \end{bmatrix}; \tag{22}$$

in cell $\boldsymbol{X}_3$:

$$\boldsymbol{A}_3 = \begin{bmatrix} -p(b+1) & p & 0 \\ 1 & -1 & 1 \\ 0 & -q & 0 \end{bmatrix}, \quad \boldsymbol{\alpha}_3 = \begin{bmatrix} p(b-a) \\ 0 \\ 0 \end{bmatrix}. \tag{23}$$

The response system is assumed to be in the form

$$\begin{aligned} &\dot{\hat{\boldsymbol{x}}}(t) = (\boldsymbol{A}_j\hat{\boldsymbol{x}}(t) + \boldsymbol{\alpha}_j) + u, \quad \hat{\boldsymbol{x}}(t) \in \boldsymbol{X}_j, \quad j = 1, 2, 3; \\ &\boldsymbol{u} = \boldsymbol{g}(\boldsymbol{y} - \hat{\boldsymbol{y}}) = \boldsymbol{g}(\boldsymbol{C}\boldsymbol{x} - \boldsymbol{C}\hat{\boldsymbol{x}}), \end{aligned} \tag{24}$$

$\boldsymbol{u} \in \boldsymbol{R}^3$ is the feedback control signals.

It is clear that the synchronisation error $\boldsymbol{e} = \hat{\boldsymbol{x}} - \boldsymbol{x}$ satisfies

$$\begin{aligned} &\dot{\boldsymbol{e}}(t) = (\boldsymbol{A}_j\hat{\boldsymbol{x}}(t) + \boldsymbol{\alpha}_j - \boldsymbol{A}_l\boldsymbol{x}(t) - \boldsymbol{\alpha}_l) + \boldsymbol{u}, \\ &\hat{\boldsymbol{x}}(t) \in \boldsymbol{X}_j, \quad \boldsymbol{x}(t) \in \boldsymbol{X}_l. \end{aligned} \tag{25}$$

Actually, according to Eq. (3), we have

$$\begin{bmatrix} \dot{e}_1 \\ \dot{e}_2 \\ \dot{e}_3 \end{bmatrix} = \begin{bmatrix} -p & p & 0 \\ 1 & -1 & 1 \\ 0 & -q & 0 \end{bmatrix} \begin{bmatrix} e_1 \\ e_2 \\ e_3 \end{bmatrix} - \begin{bmatrix} f(\hat{x}_1) - f(x_1) \\ 0 \\ 0 \end{bmatrix} + \boldsymbol{u}. \tag{26}$$

Here $f(x_1)$ is obtained from Eq. (4). For convenience, we denote $f(\hat{x}_1) - f(x_1)$ as $h(e_1, t)$. Here, $h(e_1, t)$ is time-varying because $h(e_1, t)$ does not depend only on e_1 but also on x_1 or $\hat{x}_1$ which is time-varying. But it is not difficult to find that $h(e_1, t)$ has the following relation with e_1,

$$\begin{cases} be_1 \leq h(e_1, t) \leq be_1 + 2(b-a), & e_1 \leq -2; \\ be_1 \leq h(e_1, t) \leq ae_1, & -2 \leq e_1 \leq 0; \\ ae_1 \leq h(e_1, t) \leq be_1, & 0 \leq e_1 \leq 2; \\ 2(a-b) + be_1 \leq h(e_1, t) \leq be_1, & e_1 \geq 2. \end{cases} \tag{27}$$

Which can be seen in Fig. 3.

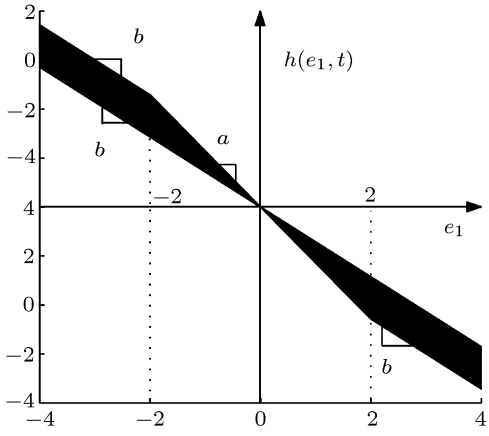


Fig. 3. Relation between $h(e_1)$ and e_1.

For $\boldsymbol{u} = \boldsymbol{0}$, we obtain the uncontrolled synchronisation error dynamics,

$$\begin{cases} \dot{e}_1(t) = p(e_2 - e_1 - h(e_1, t)), \\ \dot{e}_2(t) = e_1 - e_2 + e_3, \\ \dot{e}_3(t) = -qe_2. \end{cases} \tag{28}$$

We denote $[e_1,\ e_2,\ e_3]^{\mathrm{T}}$ as $\boldsymbol{e}$, and notice that the uncontrolled tracking error dynamics between the two piecewise-linear systems (drive and response) is actually piecewise linear and differential inclusions due to $h(e_1, t)$. We represent it by piecewise linear differential inclusions (pwLDIs) with three cell partitions, $\boldsymbol{S}_1 : \{(e_1, e_2, e_3)|e_1 \leq -2\}$, $\boldsymbol{S}_2 : \{(e_1, e_2, e_3)||e_1| \leq 2\}$ and $\boldsymbol{S}_3 : \{(e_1, e_2, e_3)|e_1 \geq 2\}$, $\boldsymbol{S}_1 \bigcup \boldsymbol{S}_2 \bigcup \boldsymbol{S}_3 = \boldsymbol{R}^3$.

$$\dot{\boldsymbol{e}}(t) = \sum_{j=1}^{J} \lambda_{lj}(t) \left(\boldsymbol{A}_{lj}\boldsymbol{e} + \boldsymbol{\alpha}_{lj}\right), \quad \boldsymbol{e}(t) \in \boldsymbol{S}_l, \tag{29}$$

where scalars $\lambda_{lj}(t) \geq 0$, $\sum\limits_{j} \lambda_{lj}(t) = 1$. There are two extreme dynamic systems $\dot{\boldsymbol{e}}(t) = (\boldsymbol{A}_{lj}\boldsymbol{e} + \boldsymbol{\alpha}_{lj})$ that define the inclusion in each cell. According to Eqs. (27) and (28), we have two extreme dynamic systems of the uncontrolled synchronisation error dynamics in cell $\boldsymbol{S}_1$:

$$\boldsymbol{A}_{11} = \begin{bmatrix} -p(b+1) & p & 0 \\ 1 & -1 & 1 \\ 0 & -q & 0 \end{bmatrix},$$

$$\boldsymbol{\alpha}_{11} = \begin{bmatrix} -2p(b-a) \\ 0 \\ 0 \end{bmatrix},$$

$$\boldsymbol{A}_{12} = \begin{bmatrix} -p(b+1) & p & 0 \\ 1 & -1 & 1 \\ 0 & -q & 0 \end{bmatrix},$$

$$\boldsymbol{\alpha}_{12} = \begin{bmatrix} 0 \\ 0 \\ 0 \end{bmatrix}; \tag{30}$$

the two extreme dynamic systems of the uncontrolled synchronisation error dynamics in cell $\boldsymbol{S}_2$:

$$\boldsymbol{A}_{21} = \begin{bmatrix} -p(a+1) & p & 0 \\ 1 & -1 & 1 \\ 0 & -q & 0 \end{bmatrix}, \quad \boldsymbol{\alpha}_{21} = \begin{bmatrix} 0 \\ 0 \\ 0 \end{bmatrix},$$

$$\boldsymbol{A}_{22} = \begin{bmatrix} -p(b+1) & p & 0 \\ 1 & -1 & 1 \\ 0 & -q & 0 \end{bmatrix}, \quad \boldsymbol{\alpha}_{22} = \begin{bmatrix} 0 \\ 0 \\ 0 \end{bmatrix}, \tag{31}$$

and the two extreme dynamic systems of the uncontrolled synchronisation error dynamics in cell $\boldsymbol{S}_3$:

$$\boldsymbol{A}_{31} = \begin{bmatrix} -p(b+1) & p & 0 \\ 1 & -1 & 1 \\ 0 & -q & 0 \end{bmatrix}, \quad \boldsymbol{\alpha}_{31} = \begin{bmatrix} 2p(b-a) \\ 0 \\ 0 \end{bmatrix},$$

$$\boldsymbol{A}_{32} = \begin{bmatrix} -p(b+1) & p & 0 \\ 1 & -1 & 1 \\ 0 & -q & 0 \end{bmatrix}, \quad \boldsymbol{\alpha}_{32} = \begin{bmatrix} 0 \\ 0 \\ 0 \end{bmatrix}. \tag{32}$$

For this uncontrolled synchronisation error dynamics, only the cell X_2 contains the origin (0,0,0). The general object of our chaos synchronisation is to find a proper feedback control law such that the closed-loop system of the synchronisation error dynamics $\dot{\boldsymbol{e}}(t) = \sum\limits_{j=1}^{J} \lambda_{lj}(t) \left(\boldsymbol{A}_{lj}\boldsymbol{e} + \boldsymbol{\alpha}_{lj}\right) + \boldsymbol{u}, \boldsymbol{e}(t) \in \boldsymbol{S}_l$ is globally asymptotically stable.

Remark 1: Although this paper only addresses the Chua's piecewise-linear chaotic model and get its pwLDIs synchronisation error model, it is believed that the similar pwLDIs synchronisation error model can be extended to more general piecewise-liner cases and even piecewise-liner hyperchaotic cases, such as hyperchaotic Chua's circuit.[39]

The simple feedback form is linear error feedback which is $\boldsymbol{u} = \boldsymbol{K}(\boldsymbol{C}\boldsymbol{x}(t) - \boldsymbol{C}\hat{\boldsymbol{x}}(t)) = -\boldsymbol{K}\boldsymbol{C}\boldsymbol{e}$. In this case, we can solve the synchronisation issue by substituting the following equations into Lemma 2 directly

$$\boldsymbol{A}_l = \boldsymbol{K},\ l = 2 \quad \bar{\boldsymbol{A}}_l = \begin{bmatrix} \boldsymbol{K}_l\boldsymbol{C} & 0 \\ 0 & 0 \end{bmatrix}, \quad l = 1, 3.$$

But noticing the property of $h(e_1, t)$, one can easily know that if the linear feedback $-KCe$ could stabilise the two extreme dynamic systems in cell S_2 simultaneously, then it can stabilise the whole error dynamics.

Naturally, considering that the error dynamics is switching according to the error dynamics state e, we should use the switching error feedback as follows:

$$\boldsymbol{u} = \boldsymbol{g}(-\boldsymbol{C}\boldsymbol{e}) = \begin{cases} -\boldsymbol{K}_l\boldsymbol{C}\boldsymbol{e}, & l = 2, \boldsymbol{e}(t) \in \boldsymbol{S}_2; \\ -\bar{\boldsymbol{K}}_l\bar{\boldsymbol{C}}\bar{\boldsymbol{e}}, & l = 1, 3, \quad \boldsymbol{e}(t) \in \boldsymbol{S}_{1,3}, \end{cases}$$

where

$$\bar{\boldsymbol{K}}_l\bar{\boldsymbol{C}} = \begin{bmatrix} \boldsymbol{K}_l\boldsymbol{C} & \boldsymbol{k}_l \\ 0 & 0 \end{bmatrix}, \quad \bar{\boldsymbol{e}} = \begin{bmatrix} \boldsymbol{e} \\ 1 \end{bmatrix}.$$

Here, $\boldsymbol{K}_l \in R^{3\times3}$ is a constant matrix and $\boldsymbol{k}_l \in \boldsymbol{R}^{3\times1}$ denotes the affine term.

Remark 2: This switching linear feedback strategy is simpler than the common nonlinear feedback and has more flexibility than the constant linear feedback to stabilise the piecewise error dynamics. Moreover, the constant linear feedback is a special case of switching feedback. It is more important that switching should provides possibility to have the lower gain being utilised when error is larger, as is desired for practical applications.

Now, the following switching linear feedback stabilisation result can be established for the synchronisation error dynamics (29–32).

Theorem 1 Consider symmetric matrices $\boldsymbol{T}$, $\boldsymbol{U}_{lj}$, and $\boldsymbol{W}_{lj}$, such that $\boldsymbol{U}_{lj}$ and $\boldsymbol{W}_{lj}$ have nonnegative entries and feedback gain matrixes $\boldsymbol{K}_l \in \boldsymbol{R}^{3\times 3}$, while

$$\bar{\boldsymbol{K}}_l\bar{\boldsymbol{C}} = \begin{bmatrix} \boldsymbol{K}_l\boldsymbol{C} & \boldsymbol{k}_l \\ 0 & 0 \end{bmatrix}, \quad l = 1, 3 \in L_1; \tag{33}$$

$$\boldsymbol{P}_l = \boldsymbol{F}_l^{\mathrm{T}}\boldsymbol{T}\boldsymbol{F}_l, \quad l = 1, 3 \in L_0; \tag{34}$$

$$\bar{\boldsymbol{P}}_l = \bar{\boldsymbol{F}}_l^{\mathrm{T}}\boldsymbol{T}\bar{\boldsymbol{F}}_l, \quad l = 2 \in L_0, \tag{35}$$

satisfy

$$0 > (\boldsymbol{A}_{lj}-\boldsymbol{K}_l\boldsymbol{C})^{\mathrm{T}}\boldsymbol{P}_l+\boldsymbol{P}_l(\boldsymbol{A}_{lj}-\boldsymbol{K}_l\boldsymbol{C})+\boldsymbol{E}_l^{\mathrm{T}}\boldsymbol{U}_{lj}\boldsymbol{E}_l = \boldsymbol{\Phi}_l, \tag{36}$$

$$0 < \boldsymbol{P}_l - \boldsymbol{E}_l^{\mathrm{T}}\boldsymbol{W}_{lj}\boldsymbol{E}_l, \tag{37}$$

for $l = 2 \in L_0$;

$$0 > (\bar{\boldsymbol{A}}_{lj}-\bar{\boldsymbol{K}}_l\bar{\boldsymbol{C}})^{\mathrm{T}}\bar{\boldsymbol{P}}_l+\bar{\boldsymbol{P}}_l(\bar{\boldsymbol{A}}_{lj}-\bar{\boldsymbol{K}}_l\bar{\boldsymbol{C}})+\bar{\boldsymbol{E}}_l^{\mathrm{T}}\boldsymbol{U}_{lj}\bar{\boldsymbol{E}}_l = \bar{\boldsymbol{\Phi}}_l, \tag{38}$$

$$0 < \bar{\boldsymbol{P}}_l - \bar{\boldsymbol{E}}_l^{\mathrm{T}}\boldsymbol{W}_{lj}\bar{\boldsymbol{E}}_l, \tag{39}$$

for $l = 1, 3 \in L_1$.

Then the switching linear feedback control: $\boldsymbol{u} = \boldsymbol{g}(-\boldsymbol{C}\boldsymbol{e})$, $\boldsymbol{e}(t) \in \boldsymbol{S}_l$ renders the piecewise linear differential inclusions (29–32) globally asymptotically stable, and consequently the drive and response chaotic Chua's circuits are globally asymptotically synchronised via switching coupled gain $\boldsymbol{K}_l$.

The proof of Theorem 1 can be easily shown by following the lemma 2 and is thus omitted. Unfortunately, it is not easy to obtain a stabilising feedback gain $\boldsymbol{K}$ from Theorem 1 directly because Theorem 1 is represented by bilinear matrix inequalities (BMIs) due to the multiplication between $\boldsymbol{K}$ and $\boldsymbol{T}$. So, we use a simpler V-K iterative algorithm for this problem.[18,19]

Algorithm 1: Initialization Step. Use pole placement design technique or any other state feedback controller design technique to determine a set of initial controller gains.

V-Step. Given a fixed controller gain $\boldsymbol{K}_l$, $l \in L_0$, $\bar{\boldsymbol{K}}_l$, $l \in L_1$, we can solve the following optimisation problem:

$$\min_{\boldsymbol{P}_l,\bar{\boldsymbol{P}}_l,\boldsymbol{U}_l,\boldsymbol{W}_l,\epsilon_l} \lambda_l$$
$$\text{s.t.}(37), (39), \boldsymbol{\phi}_l - \lambda_l\boldsymbol{I} < 0 \quad \text{and} \quad \bar{\boldsymbol{\phi}}_l - \lambda_l\boldsymbol{I} < 0$$

for a set of matrices $\boldsymbol{P}_l$, $l \in L_0$, $\bar{\boldsymbol{P}}_l$, $l \in L_1$, where $\boldsymbol{P}_l$ and $\bar{\boldsymbol{P}}_l$ are defined in Eqs. (34) and (35), $\boldsymbol{\phi}_l$ and $\bar{\boldsymbol{\phi}}_l$ are defined in Eqs. (36) and (38) respectively.

K-Step. Using the matrices $\boldsymbol{P}_l$, $\bar{\boldsymbol{P}}_l$ and ϵ_l obtained in V-Step, we solve the following optimisation problem

$$\min_{\boldsymbol{K}_l,\bar{\boldsymbol{K}}_l,\boldsymbol{U}_l,\boldsymbol{W}_l} \lambda_l$$
$$\text{s.t.}(30), (32), \boldsymbol{\phi}_l - \lambda_l\boldsymbol{I} < 0 \quad \text{and} \quad \bar{\boldsymbol{\phi}}_l - \lambda_l\boldsymbol{I} < 0$$

for a set of matrices $\boldsymbol{K}_l$, $l \in L_0$, $\bar{\boldsymbol{K}}_l$, $l \in L_1$, where $\boldsymbol{\phi}_l$ and $\bar{\boldsymbol{\phi}}_l$ are defined in Eqs. (36) and (38) respectively.

The previous iteration of V-Step and K-Step stops when $\lambda_l < 0$, $l \in L$.

4. Numerical simulations

In this section, we will carry out some numerical simulations to verify the theoretical results we have obtained. In the following, all the LMIs are solved by MATLAB LMI toolbox and all the differential equation are solved by using the fourth-fifth order Runge–Kutta method (ODE45 in MATLAB). The initial conditions of drive system are $x_1 = 0.15246$, $x_2 = -0.02281$, $x_3 = 0.38127$ and those of response system are $\hat{x}_1 = 0.2$, $\hat{x}_2 = -0.1$, $\hat{x}_3 = 0.4$ in all simulations. In order to search for the continuous piecewise quadratic Lyapunov function candidates defined in Eqs. (7) and (8), we construct $\bar{\boldsymbol{E}}_l, \bar{\boldsymbol{F}}_l$, for cells $\boldsymbol{S}_1$ and $\boldsymbol{S}_3$ and $\boldsymbol{E}_2$, $\boldsymbol{F}_2$ for cell $\boldsymbol{S}_2$ as follows:

$$\bar{\boldsymbol{E}}_1 = \begin{bmatrix} -1 & 0 & 0 & -2 \\ 0 & 0 & 0 & 1 \\ 0 & 0 & 0 & 1 \end{bmatrix}, \quad \bar{\boldsymbol{E}}_3 = \begin{bmatrix} 1 & 0 & 0 & -2 \\ 0 & 0 & 0 & 1 \\ 0 & 0 & 0 & 1 \end{bmatrix}. \tag{40}$$

$$\bar{\boldsymbol{F}}_1 = \begin{bmatrix} -1 & 0 & 0 & -2 \\ 0 & 0 & 0 & 1 \\ 0 & 0 & 0 & 1 \\ 1 & 0 & 0 & 0 \\ 0 & 1 & 0 & 0 \\ 0 & 0 & 1 & 0 \end{bmatrix}, \quad \bar{\boldsymbol{F}}_3 = \begin{bmatrix} 1 & 0 & 0 & -2 \\ 0 & 0 & 0 & 1 \\ 0 & 0 & 0 & 1 \\ 1 & 0 & 0 & 0 \\ 0 & 1 & 0 & 0 \\ 0 & 0 & 1 & 0 \end{bmatrix}. \tag{41}$$

$$\boldsymbol{E}_2 = \begin{bmatrix} 0\ 0\ 0\ 0 \\ 0\ 0\ 0\ 0 \\ 0\ 0\ 0\ 0 \end{bmatrix}, \quad \boldsymbol{F}_2 = \begin{bmatrix} 0\ 0\ 0\ 0 \\ 0\ 0\ 0\ 0 \\ 0\ 0\ 0\ 0 \\ 1\ 0\ 0\ 0 \\ 0\ 1\ 0\ 0 \\ 0\ 0\ 1\ 0 \end{bmatrix}. \tag{42}$$

In addition, $\bar{\boldsymbol{A}}_{lj}$ has the following form for cells $\boldsymbol{S}_1$ and $\boldsymbol{S}_3$

$$\bar{\boldsymbol{A}}_{lj} = \begin{bmatrix} \boldsymbol{A}_{lj} & \boldsymbol{\alpha}_{lj} \\ 0 & 0 \end{bmatrix}, \quad l = 1, 3 \in L_1. \tag{43}$$

Without loss of generality, we assume that the two state variables x_1 and x_3 are available for response system to synchronise. This means

$$\boldsymbol{C} = \begin{bmatrix} 1\ 0\ 0 \\ 0\ 0\ 0 \\ 0\ 0\ 1 \end{bmatrix}.$$

And let

$$\boldsymbol{K}_l = \begin{bmatrix} K_{l11} & 0 & 0 \\ 0 & 0 & 0 \\ 0 & 0 & K_{l33} \end{bmatrix}$$

and the affine term for cells $\boldsymbol{S}_1$ and $\boldsymbol{S}_3$: $\boldsymbol{k}_l = \begin{bmatrix} k_{l1} \\ 0 \\ 0 \end{bmatrix}$.

According to the proposed iteration algorithm 1, we obtain the result $K_{111} = K_{311} = 11.03$, $K_{133} = K_{333} = K_{233} = 8.19$, $K_{211} = 10.52$, $k_{11} = -1.02$ and $k_{31} = 1.02$ after several iterations. The synchronisation error $\|\boldsymbol{e}\| = \|\boldsymbol{x} - \hat{\boldsymbol{x}}\|$ is shown in Fig. 4. The feedback is turned on at $t = 14s$. Actually, using Theorem 1, we can verify that gains K_{111} and K_{311} can be reduced as far as to 0.8 in order to obtain lower feedback value causing by e_1 when $|e_1| > 2$. For this case, $k_{11} = -9.72$ and $k_{31} = 9.72$. The synchronisation error $\|\boldsymbol{e}\|$ is shown in Fig.5. The feedback is turned on at $t = 14$ s.

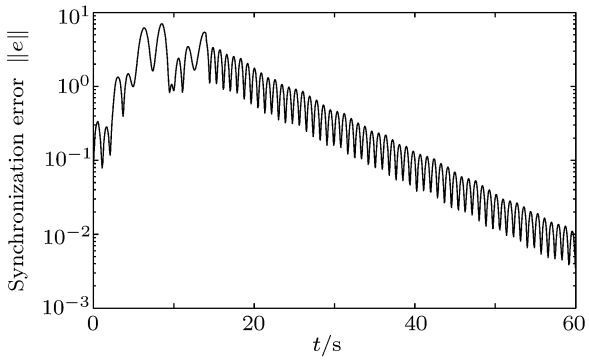


Fig. 4. Synchronisation error $|\boldsymbol{e}|$. The feedback is turned on at $t = 14$ s.

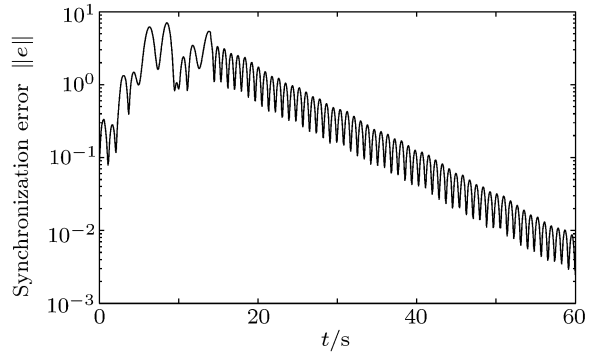


Fig. 5. Synchronisation error $|\boldsymbol{e}|$. The feedback is turned on at $t = 15$ s.

5. Conclusions

Chaotic behaviours can be found in Chua's circuit, a typical piecewise linear system. In this paper, we consider the chaos synchronisation between two unidirectional-coupled chaotic Chua's circuits. We found the piecewise linear differential inclusions (pwLDIs) model for the synchronisation error dynamics. Then we use the switching feedback to stabilise the piecewise error dynamics and drive its stabilisation conditions based on the piecewise quadratic Lyapunov function. A simpler ILMI algorithm is given to search for the coupled gain both for state feedback and output feedback. Simulation results show that this switching synchronisation scheme can achieve synchrony.

References

[1] Pecora L M and Carroll T L 1990 *Phys. Rev. Lett.* **64** 821

[2] Carroll T L and Pecora L M 1991 *IEEE Trans. Circuits Syst.* I **38** 453

[3] Ogorzalek J 1993 *IEEE Trans. Circuits Syst.* I **40** 693

[4] Hasler M and Maistrenko Y L 1997 *IEEE Trans. Circuits Syst.* I **44** 857

[5] Pecora L M, Carroll T L, Johnson G A, Mar D J and Heagy J F 1997 *Chaos* **7** 520

[6] Chen G and Dong X 1998 *From Chaos to Order Methodologies, Perspectives and Applications, ser. Nonlinear Science* (Singapore: World Scientific)

[7] Chua L O 1997 *IEEE Trans. Circuits Syst.* I **44** 927

[8] Cuomo K M, Oppenheim A V and Strogatz S H 1993 *IEEE Trans. Circuits Syst.* II **40** 626

[9] Boccaletti S, Kurths J, Osipov G, Valladares D L and Zhou C S 2002 *Physics Reports* **366** 1

[10] Yu Y B, Bao J B, Zhang H B, Zhong Q S, Liao X F and Yu J B 2008 *Chin. Phys.* B **17** 2377

[11] Yu Y B, Zhong Q S, Liao X F and Yu J B 2008 *Chin. Phys.* B **17** 842

[12] Li D and Zheng Z G 2008 *Chin. Phys.* B **17** 4009

[13] Zhang H B, Li C G, Chen G R and Gao X 2005 *Int. J. Mod. Phys.* C **16** 815

[14] Zhang H B, Liao X F and Yu J B 2005 *Chaos, Solitons and Fractals* **26** 835

[15] Zhang J, Zhang H B, Li C G and Yu J B 2004 *Chaos, Solitons and Fractals* **21** 1183

[16] Yang D S, Yu W, Zhang H G and Zhao Y 2008 *Chin. Phys.* B **17** 4056

[17] Chen S H and Kong C C 2009 *Chin. Phys.* B **18** 91

[18] Fu J, Ma T D and Zhang H G 2008 *Chin. Phys.* B **17** 4407

[19] Yang S P and Zhang R X 2008 *Chin. Phys.* B **17** 4073

[20] Han B, Han M and Niu Z Q 2008 *Acta Phys. Sin.* **57** 6824 (in Chinese)

[21] Nijmeijer H and Mareels I M Y 1997 *IEEE Trans. Circuits Syst.* I **44** 882 1997

[22] Grass G ane Mascolo S 1999 *IEEE Trans. Circuits* Syst. II **46** 478

[23] Wu C W and Chua L O 1994 *Int. J. Bifur. Chaos* **4** 979

[24] Blekhman I I, Fradkov A L, Nijmeijer H and Pogromsky A Y 1997 *Syst. Contr. Lett.* **31** 299

[25] Huijberts H J C, Nijmeijer H and Willems R M A 2000 *Int. J. Rob. Nonlin. Contr.* **10** 363

[26] Nijmeijer H A 2001 *Physica* D **154** 219

[27] Jiang G P and Tang K S 2002 *Int. J. Bifur.Chaos* **12** 2239

[28] Feng G 2002 *IEEE Trans. CAS* **49** 224

[29] Mulder E F and Kothare M V 2000 *Proceeding of the American Control Conference* Chicago, Illinois p4813

[30] Zhang H B, Li C G and Liao X F 2005 *Int. J. Mod. Phys.* B **19** 4389

[31] Zhang H B, Li C G, Zhang J, Liao X F and Yu J B 2005 *Chaos, Solitons and Fractals* **22** 1053

[32] Chua L O 1985 *IEEE Trans. Circuits Syst.* I **32** 797

[33] Johansson M and Rantzer A 1998 *IEEE Trans. Automat. Contr.* **43** 555

[34] Johansson M 2003 *Piecewise Linear Control Systems* (Singapore-Verlag Berlin Heidelberg)

[35] Zhang H B, Li C G and Liao X F 2006 *IEEE Trans. SMC-B* **36** 685

[36] Zhang H B and Feng G 2008 *IEEE Trans. SMC-B* **38** 1390

[37] Zhang H B 2008 *IEEE Trans. Fuzzy Systems* **14** 1649

[38] Boyd S, Ghaoui L, Feron E and Balakrishnan V 1994 *Linear Matrix Inequalities in System and Control Therory* (Philadelphia: SIAM)

[39] Matsumoto T, Chua L O and Kobayashi K 1986 *IEEE Trans. Circuits Syst.* **33** 1143